Available online at www.sciencedirect.com

ScienceDirect

Procedia Structural Integrity 2 (2016) 855–862

Structural Integrity Procedia

www.elsevier.com/locate/procedia

21st European Conference on Fracture, ECF21, 20-24 June 2016, Catania, Italy

Creep-fatigue crack growth behaviour of P91 steels

N. Ab Razak[a,b,]* ,C.M. Davies[a], K.M. Nikbin[a]

[a]*Department of Mechanical Engineering, Imperial College London, London SW7 2AZ, United Kingdom*
[b]*Department of Mechanical Engineering, University Malaysia Pahang, Pekan Pahang 26600, Malaysia*

Abstract

The importance of predicting failure due to combined creep-fatigue crack growth in high temperature power-plant components has become of great importance importance due to the need for plant to 'load follow' in response to fluctuations in demands and the availability of renewables. P91 steel has been widely utilized in conventional plant components. Creep fatigue crack growth (CFCG) tests have been performed on compact specimens at temperatures ranging between 600° C to 625° C. The experimental results have been compared to static creep, high cycle fatigue and CFCG test data available in literature on P91 steel. The CFCG data has been characterised using stress intensity factor range parameter, ΔK and C^* parameter. The crack growth per cycle and ΔK relationship shows that at high frequency, the CFCG behaviour tends to that of high cycle fatigue crack growth and at low frequency, the contribution of creep becomes increasingly more significant. The correlation between crack growth rate and C^* parameter, shows that most CFCG data fall within the creep crack growth (CCG) P91 data band which may indicate that the crack growth behaviour is dominated by creep processes. Fractography has also shown an intergranular, ductile fracture surface indicating creep dominance for the conditions considered. A linear cummulative rule has ben used to predict the CFCG experimental result.

Peer-review under responsibility of the Scientific Committee of ECF21.

Keywords: Creep fatigue; Crack Growth behaviour; P91 steel

* Corresponding author. Tel.: +44 20 7594 7133
E-mail address: n.ab-razak13@imperial.ac.uk

Copyright © 2016 The Authors. Published by Elsevier B.V. This is an open access article under the CC BY-NC-ND license (http://creativecommons.org/licenses/by-nc-nd/4.0/).
Peer review under responsibility of the Scientific Committee of ECF21.
10.1016/j.prostr.2016.06.110

1. Introduction

Many conventional power plants are increasingly required to operate in a 'flexible' manner in response to the availability of renewable energy, though generally designed to operate at base loads. This flexible operation implies that the mechanical and thermal loads on high temperature components are cyclic. This cyclic operation may lead to interactive creep-fatigue failure mechanisms taking place that is known to accelerate failure compared to static creep loads alone. Therefore it is imperative that the creep-fatigue crack growth behavior of power-plant components are characterized and understood.

The creep fatigue crack growth (CFCG) behaviour of engineering alloys have been investigated by a number of researchers (Lu et al. (2006), Narasimhachary and Saxena (2013), Bassi et al. (2015), Mehmanparast et al. (2011), Holdsworth (2011), Granacher et al. (2001)). Lu et al. (2006) investigated the effect of temperature and hold time on the CFCG behaviour of a nickel based superalloy and showed that as the hold time increase, the crack growth behavior changed from cycle dependent to time dependent behavior. This transition occurred at a smaller hold time as the test temperature was increased. Bassi et al. (2015) conducted CFCG tests on T/P91 power plant steel and employed a simple superposition approach to sum creep and fatigue damage contributions and predict the CFCG behavior. The results show that under creep-fatigue loading conditions with a holding time 0.1 h, the crack growth behavior is as a pure fatigue crack growth (FCG) test. For hold times between 1 and 10 h, the crack growth behaves as a pure creep crack growth (CCG) test, whereas for hold times between 0.1 and 1 h interactive CFCG behavior was observed. The CFCG behavior on four type of steels namely, 316L, 1CrMoV, P91 and P22, which were tested at a range of frequencies was examined by Mehmanparast et al. (2011) who found that for a cyclic frequency below 0.1 Hz, the crack growth behavior was time dependent and was correlated with the creep fracture mechanics parameter C^*. A simple linear cumulative rule was also used to describe the effects of creep-fatigue interaction on the crack growth rates.

In this work an experimental analysis of CFCG has been performed on P91 steel. CFCG tests have been performed on compact tension, C(T), samples at a range of temperatures between 600°C and 625 °C for a hold time of 600 s. Tests have been performed on two ex-service materials and an unused as-received (AR) material. The crack growth behavior has been correlated with the stress intensity factor range, ΔK, and the C^* parameter. The results are compared to a range of FCG, CCG and CFCG test data found in the literature (Mehmanparast et al. (2011), Narasimhachary and Saxena (2013), Granacher et al. (2001), Speicher.M et al. (2013)). Fractography was performed on fracture surface to identify the dominant failure mechanism and linear cumulative rule approach employed to predict results obtained.

2. Material

The properties of the three P91 steels tested in this work are shown in Table 1. Note that hereon for brevity, the as-received material is denoted 'P91-A'. Of the two ex-service P91 steel materials tested, one was previously in operation for over 110,000 hours at 590°C (denoted P91-B) and the other at 600°C for over 100,00 hours (denoted P91-C). Metallographic analysis has been performed on the as-received material P91-A and the ex-service material P91-B, as shown in Figure 1, where the materials was etched using Villela agent (containing 1g of picric acid, 5ml of HCI and 100 ml of ethanol). Similar microstructures are seen in both as received and ex-service materials where the expected lath martensite microstructure is observed.

Table 1. Material properties of P91 material at room and elevated temperature

Material ID	Material Condition	Temperature (°C)	σ_{YS} (MPa)	σ_{UTS} (MPa)	E (GPa)	% Tensile Elongation
A	As-received	25	570	663	203	-
B	Ex-service	25	-	665	-	-
C	Ex-service	25	533	708	220	26
A	As-received	620	340	360	127	-
B	Ex-service	600	-	-	-	-
C	Ex-service	625	325	344	125	33

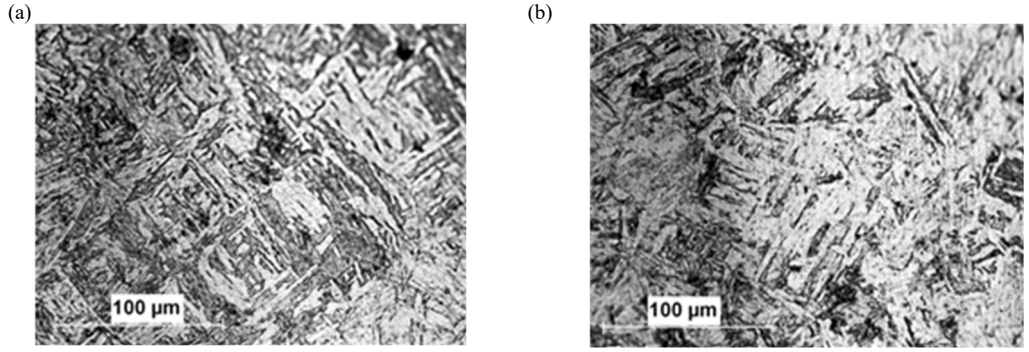

Fig.1. Microstructure of P91 in a) as-received condition (P91-A) ;b) Ex- service condition (P91-B)

3. Experimental Testing

Creep-fatigue crack growth testing has been performed according to the testing standard, ASTM E-2760 (ASTM (2010)). Four C(T) samples have been tested, as detailed in Table 2. One from the as-received material P91-A, identified as CT-A, one from the ex-service materiel P91-B, identified as CT-B and two from the ex-service material P91-C, identified as CT-C1 and CT-C2. Note that test specimens CT-C1 and CT-C2 contributed to a larger ASTM organised round robin project, as detailed in Saxena and Narasimhachary (2014), Kalyanasundaram et al. (2011). CT-C1 and CT-C2 were fatigue pre-cracking to an initial crack length to width ratio, $a_0/W \sim 0.4$ at room temperature, whereas CT-A and CT-B were electrical discharge machining (EDM) notched with a wire diameter of 0.25 mm. All C(T) specimens were then side grooved by 10% of the specimen thickness on each side, to produce a uniform crack growth.

The CFCG testing was performed on a creep machine using pneumatic load-lifting equipment. The direct current potential drop (PD) technique was utilized to continuously monitor the crack length, employing a linear calibration, (ASTM, 2010) and a linear variable differential transformer (LVDT) was used to monitor the load line displacement (LLD). A triangular waveform was used and loading and unloading times were held constant (approximately 2s load and unload times). Hold time of duration of 600s were superimposed on the maximum load. All tests were performed at 600°C, 620°C and 625°C (see Table 2) at a load ratio, R of 0.1. The test were interrupted prior to full fracture and subsequently broken open at room temperature by high frequency fatigue loading. The initial crack length, a_0 , and the final crack length, a_f , were then calculated by averaging 9 measurements along the crack front (ASTM (2010)).

Table 2. Creep fatigue test condition

Specimen ID	Material Condition	T (°C)	B (mm)	a_0/W	Max.load (kN)	Initial ΔK (MPa√m)	Initial a (mm)	Final ΔK (MPa√m)	Final a (mm)
CT-A	As-received	620	25.0	0.45	15.0	22.5	22.5	38.4	30.5
CT-B	Ex-service	600	25.0	0.50	13.0	22.6	25.0	28.9	28.7
CT-C1	Ex-service	625	12.5	0.42	7.5	20.5	20.8	31.6	27.9
CT-C2	Ex-service	625	12.5	0.44	9.0	25.9	21.8	37.9	27.9

4. Correlation of crack growth and creep deformation

Under fatigue control condition, the crack growth rate per cycle, da/dN can be described by Paris law (Paris and Erdogan (1963)) which can be expressed as

$$da/dN = \lambda \Delta K^{p} \tag{1}$$

where λ and p is a material constant. The creep parameter C^* can be determined experimentally using Davies et al. (2006)

$$C^* = \frac{P\dot{\Delta}}{B(W-a)}H\eta \tag{2}$$

where P is the applied load, and $\dot{\Delta}$ is load line displacement. H and η is a dimensionless coefficient that depends on specimen geometry. For a C(T) specimen, $H = n/(n+1)$ and $\eta = 2.2$, where n is the power-law creep exponent. The crack growth rate and C^* under steady state condition can be represented as

$$\dot{a} = DC^{*\phi} \tag{3}$$

where D and ϕ are the CCG power-law coefficient and exponent respectively. The CCG rate for a given value of C^* can be estimated using the approximate NSW crack growth model (NSWA) (Nikbin et al. (1986)) given by

$$\dot{a}_{NSWA} = \frac{3C^{*0.85}}{\varepsilon_f^*} \tag{4}$$

where ε_f^* is the multiaxial creep ductility which is usually taken as uniaxial creep failure strain, ε_f for plane stress condition and $\varepsilon_f/30$ for plane strain condition (Tan et al. (2001)).

The total crack growth per cycle is contributed by the cyclic dependent component and the time dependent component, which can be expressed as a linear summation

$$\left(\frac{da}{dN}\right)_{total} = \left(\frac{da}{dN}\right)_{fatigue} + \frac{(da/dt)_{creep}}{3600f} \tag{5}$$

where f is the frequency of load cycle in Hz. The fatigue crack growth rate in Eq (1) and creep crack growth rate in Eq (3) can be substituted into Eq (9) and may expressed as

$$\left(\frac{da}{dN}\right)_{total} = \lambda\Delta K^p + \frac{DC^{*\varphi}}{3600f} \tag{6}$$

where the first term on the right hand side of Eqn (6) gives the contribution from the cyclic (fatigue) component and the second the contribution from the time dependent (creep) process.

5. Result and discussion

5.1. Crack growth correlation with the stress intensity factor range

Figure 3(a) compares the crack extension, Δa, against number of cycles normalized by the number of cycles to failure, N/N_f and Figure 3 (b) shows the load line displacement (LLD) relationship against time normalized by tests duration for all specimens tested. Note that the tests duration is subjective to the point where the test was interrupted, which corresponded to a point of acceleration in crack growth rate. As expected, CT-C2, which was subjected to the highest load and temperature, had the shortest test duration. In addition CT-C2 appears to have an initiation period before significant crack growth has occurred, however all other tests show steady growth from initial loading. Considering the applied load and temperature, CT-A had a significantly longer test duration than the ex-service material and a large LLD and crack extension prior to test completion, which may be due to thermal aging or creep damage accumulation effects in the ex-service material.

Figure 4 shows the crack growth rate per cycle, da/dN, correlated with the stress intensity factor range, ΔK. In order to investigate the effect of various frequencies on the CFCG growth behavior, data from literature (Mehmanparast et al. (2011), Speicher.M et al. (2013), Granacher et al. (2001), Narasimhachary and Saxena (2013)) have been included in Fig. 4. The dashed and dotted line illustrates the regression fit made to the data with a frequency less than 0.002 Hz and between 0.01 and 1 Hz. At frequencies >0.01 Hz, the CFCG behaviour tends to that of high cycle fatigue crack growth and data for all temperatures considered fall close to each other. At lower frequencies, the crack growth rate progressively increases with a decreasing in frequency and an increase in temperature, due to a significant creep contribution.

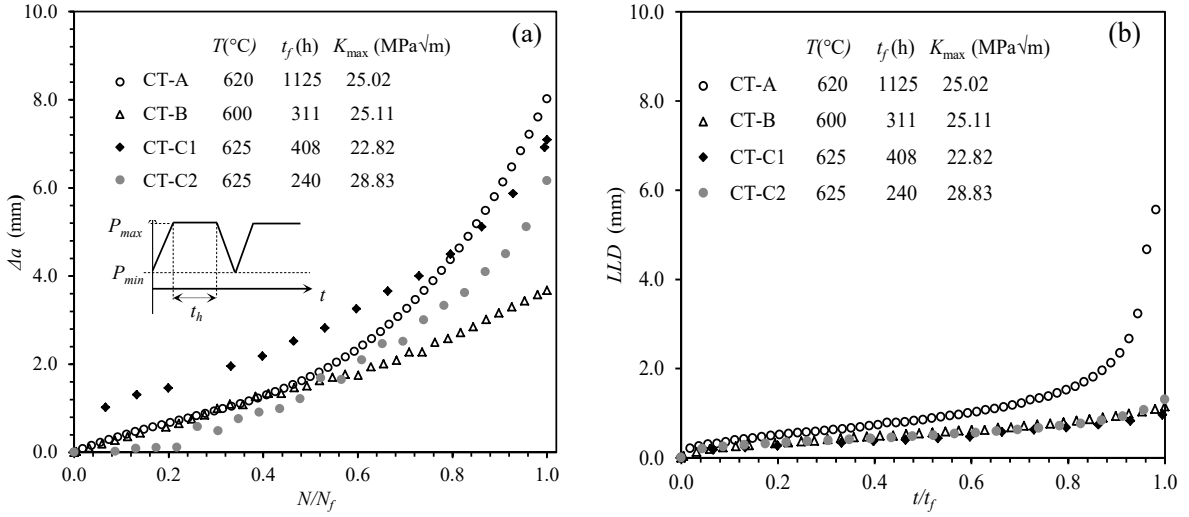

Fig.3. (a) Crack extension versus normalized number of cycles; b) Load line displacement versus normalized time

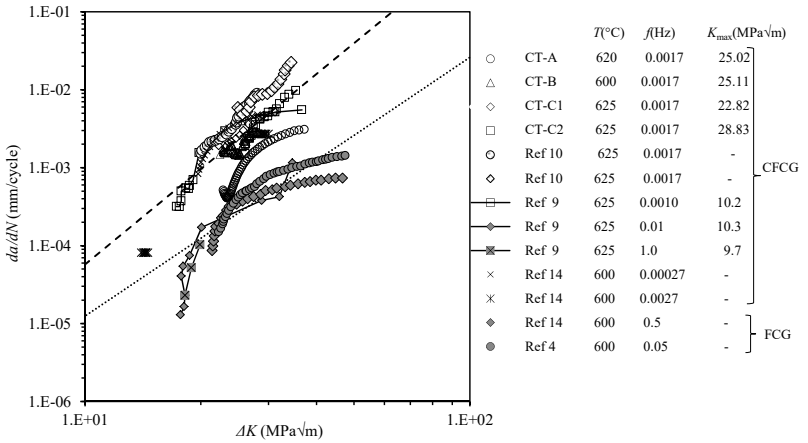

Fig.4. Crack growth for P91 steel at various cyclic frequencies

5.2. Crack growth correlation with the C parameter*

The CFCG test data has been correlated with the C^* parameter and compared with available static creep crack growth (CCG) data for P91 steel in the temperature range 600°C to 625°C from literature Speicher.M et al. (2013), Maleki (2015), Mehmanparast et al. (2011), as shown in Figure 5. P91 CCG scatter data band at 580°C to 625°C and predictive NSWA model (Eqn 8) has been plotted in Fig.5. A power-law creep exponent of $n = 8.24$ (Narasimhachary and Saxena, 2013) and a uniaxial failure strain of 33% has been used in the NSWA model. In Fig. 5 the closed symbols refer to CFCG data whilst the open symbol indicate the static CCG data. It is apparent that the CFCG data fall into the same scatter band as the static CCG data (Maleki (2015), Speicher.M et al. (2013)), however the CFCG data generally falls towards the upper bound of the static CCG data and there is some indication that an increase in temperature results in a high crack grwoth rate. The CFCG data are mostly bounded by the NSWA prediction line, however the plane strain NSWA model overly predicts the crack growth rate.

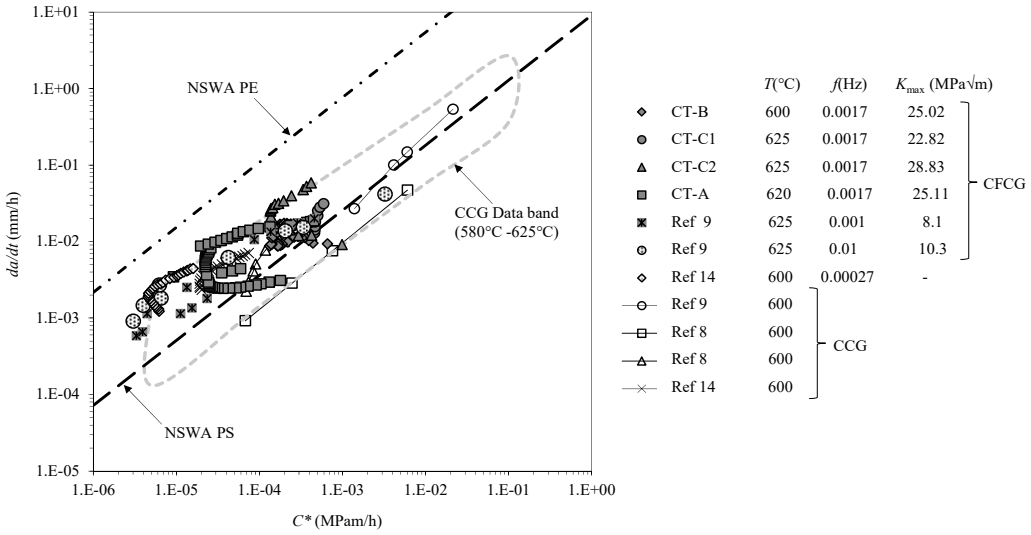

Fig.5. Correlation of creep fatigue crack growth data, creep crack growth data and predictive NSWA model for P91 material.

5.3. Creep-fatigue interaction

The frequency dependence of CFCG behaviour can be predicted using Eqn (6) where the constants, determined from static CCG and high frequency FCG testing Webster (1994), are D = 6.5 and φ = 0.7 (Maleki (2015)) and λ =1.5×10-8, p = 3.57, (Mehmanparast et al. (2011)). Figure 6 shows the frequency dependence of crack growth per cycle for P91 steel for ΔK = 30 MPa√m and also literature data for ΔK = 20 MPa√m, which correspond to values of ΔK that fall in the Paris law FCG region for the tests considered. At high frequencies, fatigue is the dominant mechanism and the crack growth per cycle is insensitive to frequency, as shown by the horizontal line. At low frequencies, creep is expected to dominate leading to intergranular fracture. At intermediate frequencies (approx. 0.1 Hz) both fatigue and creep process are significant and mixed intergranular and transgranular fracture is expected. As explained in (Webster, 1994) both types of process are likely to develop intermittently through or around individual grains. Hence, at intermediate frequencies when one mechanism becomes arrested locally, the other may take over to allow cracking to progress at a rate equal to the sum of individual rate (Webster, 1994). It can be seen that at a frequency of 0.0017 Hz, the CFCG data falls within the region that is expected to be creep dominant, leading to intergranular failure.

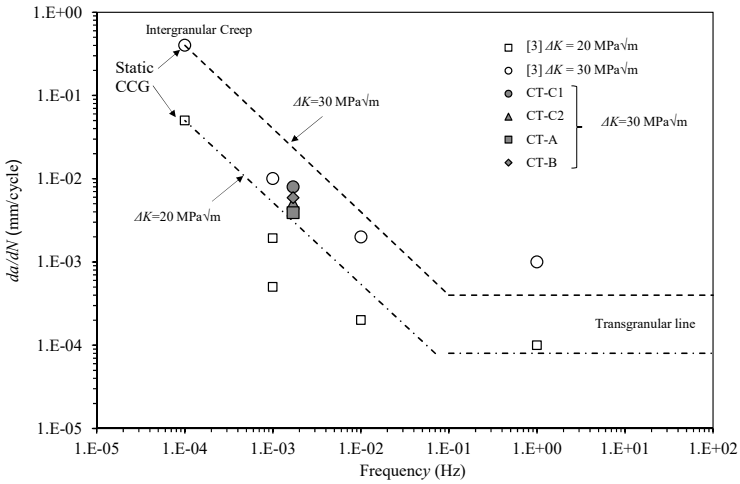

Fig.6. Frequency dependence of crack growth per cycle for P91 material

5.4. Fractography

Prior to breaking open the specimens, a 3 mm slice was extracted from the mid thickness of the sample to examine the fracture path. Figure 7 (a-c) shows an optical microscopy of the fracture paths of samples CT-B, CT-C1 and CT-A, respectively. The crack path in the ex-service material sample CT-B (Fig.7 a) is relatively straight fronted, with a number of small branches from the main crack. In Fig.7 (b) the cracking behaviour of CT-C1 ex-service material, the initial fatigue pre-crack is relatively straight, however in the CFCG region the crack grows at an angle. However for the as-received specimen CT-A, Fig.7 (c), a large crack opening displacement is observed, which is consistent with Figure 3(b), and the crack shows some discontinuous branching, signifying that the crack growth is creep dominated.

The fracture surface of sample CT-A has been examined in more detail using the scanning electron microscope (SEM). Figure 8(a) shows a macrograph of the fracture surface where it is clear that the creep fatigue crack growth region is faceted, and in comparison the FCG region (used to break open the sample) is relatively flat. The SEM images from these two regions are shown in Fig. 8 (a) and (b). The CFCG region, Fig. 8 (a), appears to be intergranular when compared to the transgranular fatigue dominant region in Fig. 8 (b). Though not shown, similar SEM observations were seen in samples CT-B, CT-C1 and CT-C2.

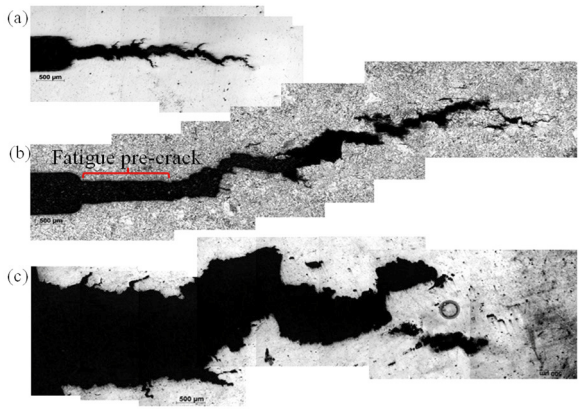

Fig.7. Cracking behaviour of (a) CT-B; (b) CT-C1; (c) CT-A

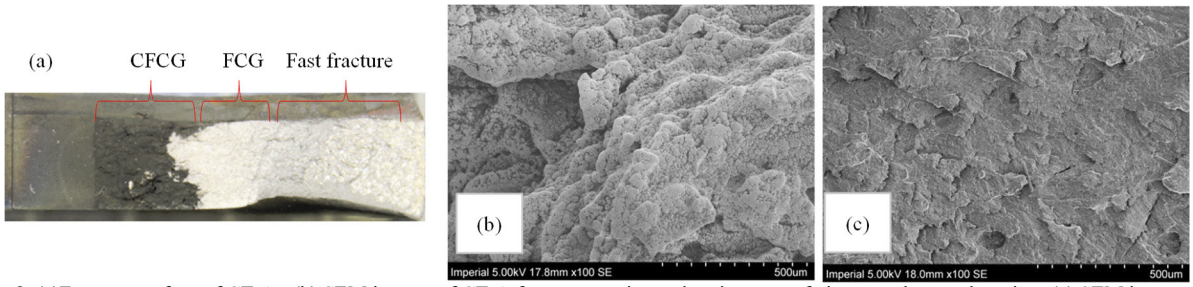

Fig.8. (a)Fracture surface of CT-A ; (b) SEM images of CT-A fracture specimen showing creep fatigue crack growth region ;(c) SEM images of CT-A fracture specimen showing fatigue crack growth region

6. Conclusion

The creep fatigue crack growth behaviour of P91 steel in as-received and ex-service material conditions has been examined. The crack growth data was characterized using fracture mechanics parameters ΔK and C^*. The results showed that at high frequency (> 0.01 Hz), the CFCG behaviour tend to that of high cycle fatigue crack growth and is best correlated with the ΔK parameter whereas at lower frequencies, creep mechanisms have been found to dominant and best correlated with the C^* parameter. The correlation between crack growth rate and C^* parameter,

shows that most of the CFCG tested at 600°C to 625°C fall within the CCG P91 scatter band data for this temperature range. A linear cumulative rule approach has been used to predict the CFCG experimental result by considering the frequency effect. The data has been found to be relatively consistent with the prediction lines. An intergranular fracture surface was observed for all CFCG tests examined with a frequency of less than 0.002 indicating that the fracture process is creep dominant.

Acknowledgements

The authors would like to acknowledgements the financial support by Ministry of Higher Education of Malaysia.

References

ASTM E2760.2010." Standard Test Method for Creep Fatigue Crack Growth Testing *Annual Book of ASTM Standards* Vol.03.01. ASTM International,West Conshohocken,PA,pp.1012-1035

Bassi, F., Foletti, S. & Conte, A. L., 2015. Creep Fatigue Crack Growth and Fracture Mechanism at T/P91 Power Plant Steel. Materials at High Temperatures(32:3):250-255.

Davies, C., Kourmpetis, M., Dowd, N. & Nikbin, K., 2006. Experimental Evaluation of the *J* or *C** Parameter for a Range of Cracked Geometries. Journal of ASTM International 3(4). DOI: 10.1520/STP45541S

Granacher, J., Klenk, A., Tramer, M., Schellenberg, G., Mueller, F. & Ewald, J., 2001. Creep fatigue crack behavior of two power plant steels. International Journal of Pressure Vessels and Piping 78(11–12):909-920.

Holdsworth, S. R., 2011. Creep Fatigue Interaction in Power Plant Steels. Materials at High Temperatures(28:3):197-204.

Kalyanasundaram, V., Saxena, A., Narasimhachary, S., & Dogan, B., 2011. ASTM Round-Robin on Creep Fatigue and Creep Behaviour of P91 Steel. Jounal of ASTM International 8(4).

Lu, Y. L., Chen, L. J., Liaw, P. K., Wang, G. Y., Brooks, C. R., Thompson, S. A., Blust, J. W., Browning, P. F., Bhattacharya, A. K., Aurrecoechea, J. M. & Klarstrom, D. L., 2006. Effects of temperature and hold time on creep-fatigue crack-growth behavior of HAYNES® 230® alloy. *Materials Science and Engineering* **429(1–2)**:1-10.

Maleki, S., 2015. Long Term Creep Deformation and Crack Growth Predictions for Grade 91 steels and Risk Based Methods in Their Component Life Assessment.) Imperial College London, PhD.

Mehmanparast, A., Davies, C. M. & Nikbin, K. M., 2011. Evaluation of Testing and Analysis Methods in ASTM E2760-10 Creep-Fatigue Crack Growth Testing Standard for a Range of Steels. DOI: 10.1520/JAI103602

Narasimhachary, S. B. & Saxena, A., 2013. Crack growth behavior of 9Cr−1Mo (P91) steel under creep–fatigue conditions. International Journal of Fatigue 56(0):106-113.

Nikbin, K. M., Smith, D. J. & Webster, G. A., 1986. An Engineering Approach to the Prediction of Creep Crack Growth. Journal of Engineering Materials and Technology 108(2):186-191.

Paris, P. & Erdogan, F., 1963. A Critical Analysis of Crack Propagation Laws. Journal of Basic Engineering 85(4):528-533.

Saxena, A. & Narasimhachary, S. B., 2014. Round robin on creep fatigue crack growth testing for verification of ASTM standard 2760-10. *Materials at High Temperatures* 31(4):357-363.

Speicher.M, Klenk, A. & Coleman.K., 2013. Creep Fatigue Interactions in P91 Steel. Proceeding of 13th International Conference on Fracture June 16-21 in Beijing,Chine.

Tan, M., Celard, N. J. C., Nikbin, K. M. & Webster, G. A., 2001. Comparison of creep crack initiation and growth in four steels tested in HIDA. International Journal of Pressure Vessels and Piping 78(11–12):737-747.

Webster, G. A. and and Ainsworth, R.A., High Temperature Component Life Assessment. 1st ed,Chapman and Hall, London, 1994 .